Title: Copper as a Novel Regulator of PERK

Authors: Sarah E. Bond[1], Noah R. Beratan[2], Margaret K. Bond[2], Donita C. Brady[3], Kelly L. Jordan-Sciutto[2]

Affiliations:
1) Department of Biochemistry and Biophysics, Perelman School of Medicine, University of Pennsylvania
2) Department of Oral Medicine, School of Dental Medicine, University of Pennsylvania
3) Department of Cancer Biology, Perelman School of Medicine, University of Pennsylvania,

Abstract

PERK is a transmembrane kinase located on the ER with a luminal domain that senses ER stresses, such as protein misfolding, and a cytosolic kinase domain. Upon stress sensing, PERK activates and phosphorylates eIF2α to attenuate global translation while upregulating select transcripts to re-establish protein homeostasis. In a secondary phase of signaling PERK can also induce apoptosis to dispose of terminally stressed and damaged cells. Thus, the delineated bi-phasic nature of PERK signaling requires tight regulation for homeostatic function, as evidenced by dysregulation of this pathway being implicated in many diseases, including cancers and neurodegenerative conditions. Pursuant attempts to therapeutically modulate PERK and its signaling outcomes have highlighted that our understanding of the determinants of adaptive vs. mal-adaptive signaling remain ambiguous, and further delineation of PERK regulation is required. Here we report copper as a regulator of PERK kinase activity. PERK copper binding activity was confirmed by selective affinity for a copper charged resin and by ICP-MS quantification of bound copper. Mutation of the putative copper binding site, identified based on homology, abolished copper binding. Copper-binding was also determined to be necessary for kinase activity in *in vitro* kinase assays. Physiologic manipulation of copper availability in cells modulated PERK activity and signaling. Using this relationship, we show that copper availability determines ER stress tolerance and cell fate outcomes. This novel regulatory mechanism has broad implications for modulation of PERK activity in different diseases and

disease models, and may constitute a previously unaccounted for variable in determining when PERK inhibition vs activation is therapeutically beneficial.

1. Introduction

Pancreatic/PKR-like endoplasmic reticulum kinase (PERK) is a kinase responsible for phosphorylating the alpha subunit of eukaryotic initiation factor 2 (eIF2α) in response to the accumulation of unfolded proteins and other ER stressors (Hetz and Papa, 2018). PERK is one of four eIF2α kinases, the others being Protein kinase RNA-activated (PKR), General Control Nonderepressible 2 (GCN2), and Heme-regulated inhibitor (HRI), which respond to specific cellular stresses, viral infection, amino acid deprivation, and heme insufficiency, respectively, to make up the integrated stress response (ISR) (Bond et al., 2020). PERK responds to ER stress as part of a greater stress signaling network, called the Unfolded Protein Response (UPR) that is activated upon ER stress to re-establish protein homeostasis (Noack et al., 2014). Specifically phosphorylation of eIF2α by PERK results in global protein translation attenuation, with selective upregulation of transcripts encoding factors that mitigate stress, such as protein chaperones, as well as in induction of the antioxidant response by PERK phosphorylation of the transcription factor Nrf2 (Hetz and Papa, 2018; Walter and Ron, 2011). However, with prolonged or severe stress, subsequent signaling steps result in the induction of cell death, to dispose of terminally stressed and damaged cells (Urra et al., 2013). Contrarily, ablation of PERK signaling can also result in cell death via unresolved ER stress on the front end, and enhanced PERK activity has been shown to result in increased ER stress tolerance in some contexts (Shacham et al., 2021). PERK has thus been seen to act beneficially in a narrow range of activity that is tightly regulated, and dysregulation of this signaling cascade has been proposed to play a role in many pathologies, including neurodegenerative diseases, and cancers. Based on conflicting findings where either PERK inhibition or activation can be either

beneficial or detrimental, depending on the stress context, there is a need for better understanding of PERK regulation and its downstream outcomes.

Copper has a long history of vital involvement in human physiology, as well as pathophysiology, but classically, these roles have been attributed to its loading into essential proteins as a static cofactor, and its toxicity in its free form (Grubman and White, 2014; Kardos et al., 2018). However, in more recent years there has been growing evidence of a pool of "labile" lightly bound copper, which can be mobilized during signaling events to transiently affect protein function (Tsang et al., 2021). Turski et al. characterized the first copper-regulated kinases, Mitogen activated kinase Kinases 1 and 2 (MEK1/2), as being able to bind and be reversibly regulated by copper. In a series of studies they specifically delineated the residues involved in copper binding as well as the copper binding affinity and stoichiometry of MEK. In follow-up they demonstrated that copper binding is required for MEK activity, such that copper manipulations, including chelation, could be used to modulate MEK1/2 activity, including to therapeutic benefit in cancer models (Brady et al., 2014; Grasso et al., 2020; Grasso et al., 2021; Turski et al., 2012).

Following the initial characterization of MEK1/2, several other kinases and other enzymes, including Unc-51 Like autophagy activating Kinases 1 and 2 (ULK1/2), Pyruvate Dehydrogenase Kinase 1 (PDK1), Phosphodiesterase 3B (PDE3B), a clade of ubiquitin-conjugating enzymes (UBE2D), and the histone H3-H4 tetramer have been characterized to bind and be regulated by copper binding (Attar et al., 2020; Guo et al., 2021; Krishnamoorthy et al., 2016; Opazo et al., 2021; Tsang et al., 2020). The autophagic kinase ULK1/2 was specifically investigated in follow up studies from the identification of MEK1/2 to identify the copper kinome using tri-faceted screen: 1) Pull-down from whole cell lysate with copper charged resin; 2) Inhibition with the copper chelator tetrathiolmolybdate (TTM) in an *in vitro* kinase assay; 3) Sequence homology with the putative copper binding sites identified in MEK1/2. Another potential copper regulated kinase identified by these screens was PERK. Here we present

evidence that PERK activity is in fact regulated by copper binding. Specifically PERK binds copper in a putative binding site-dependent manner, and this binding is necessary for kinase activity. Furthermore, PERK activity can be modulated *in vitro* and in cells in a dose-dependent manner using copper chelators and genetic manipulations of copper homeostasis. We have evidence that this relationship can also be used to modulate ER stress tolerance and cell fate outcomes via copper manipulation. This novel regulatory mechanism has broad implications for modulating PERK activity in different diseases and disease models, and may constitute a previously unaccounted for variable in determining when PERK inhibition vs. activation would be therapeutically beneficial.

2. Results

2.1 PERK binds copper near the kinase active site

PERK was found to bind a copper charged column and to be inhibited by the copper chelator tetrathiomolybdate (TTM) in a kinase activity screen in preliminary screening experiments. To follow up on these findings, we first assessed whether PERK is able to interact with copper via its ability to be pulled down from mouse embryonic fibroblast (MEF) whole cell lysate using metal-loaded immobilized metal affinity chromatography (IMAC) resin. As shown in **Figure 1A**, PERK was selectively pulled down by copper charged IMAC resin, as opposed to uncharged or zinc-charged resin, and to other cellular protein such as Actin. To determine whether this interaction was direct, or required cellular mediators, purified recombinant GST-tagged PERK kinase domain was also assessed for interaction with the differently charged IMAC columns. As shown in **Figure 1B**, purified PERK was again selectively pulled down by the copper-charged copper column, and not by the uncharged resin. PERK also showed binding interaction with zinc charged resin in this assay, though this interaction was weak enough for some elution of bound protein in the wash step.

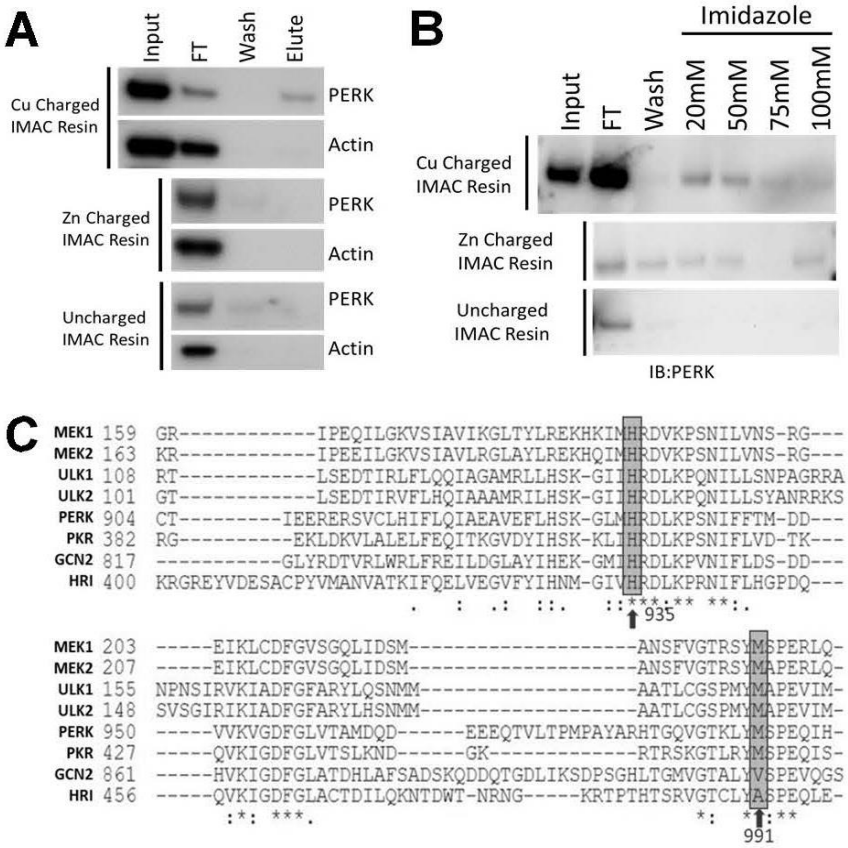

Figure 1-PERK Binds Copper

A) Western blot images, probed as indicated, of pulled-down protein from charged IMAC resin incubated with MEF whole cell lysate. Wash=Binding buffer + 20mM imidazole. Elute=Binding buffer + 100mM imidazole.

B) Western blot images, probed as indicated of pulled-down protein from charged IMAC resin incubated with purified protein.

C) Alignment of PERK amino acid sequence with other eIF2α kinases and previously characterized copper binding proteins MEK1/2 and ULK1/2. Putative copper binding residues are outlined.

D) Table dictating putative copper binding residues by homology.

E) ICP-MS results showing copper content of submitted samples, adjusted for buffer content, and calculated concentration.

F) Western blot images, probed as indicated, of pulled-down protein from glutathione sepharose resin incubated with indicated purified protein.

IMAC=Immobilized Metal Affinity Chromatography; MEF=Mouse Embryonic Fibroblast; ICP-MS=Inductively

To determine the residues coordinating copper binding, we mutated PERK's putative copper binding site, based on alignment with previously characterized copper binding proteins (**Figure 1C-D).** Specifically histidine 935 and methionine 991 were mutated to alanine to form the copper binding mutant (CBM). These mutations were introduced by site-directed mutagenesis into C-terminal FLAG tagged full-length and kinase domain PERK constructs, which were then expressed and purified in parallel with unmutated protein (**Supplemental Figure 1A**). To confirm the copper bound status and binding ability of our purified constructs, kinase domain PERK and its copper binding mutant were submitted for ICP-MS as purified, as well as following a copper incubation protocol. Copper quantification of the samples was used to determine copper occupancy of the protein (**Supplemental Figure 1C, Figure 1E**). Samples were submitted at a measured 10uM protein, however, Coomassie staining showed some contaminants in the purified protein product (**Supplemental Figure 1B**) that prevented absolute quantification of PERK. Nonetheless, PERK kinase domain as purified and found to bind copper with an estimated stoichiometry as low as one copper atom per ten PERK molecules, which could be increased by incubation with glutathione complexed copper to 1:2 copper:PERK, assuming 10uM PERK (**Figure 1E**). The copper binding mutant on the other had no detectable copper bound, as purified. In line with these findings, the purified PERK kinase domain was found to be pulled-down by glutathione sepharose, which is known to be able to bind copper, whereas the CBM showed no interaction (**Figure 1F**). These results indicate the PERK is able to bind copper directly both in the cellular environment and *in vitro*, and that residues Histidine 935 and Methionine 991 together are required for this binding.

2.2 PERK-copper binding is required for kinase activity

After determining PERK's copper binding activity, we next sought to test whether this binding regulated kinase activity, given the proximity of the identified binding site to the kinase catalytic site. Indeed, as seen in **Figure 2A-B**, under conditions where PERK kinase activity

was observed to be linear over time *in vitro* (**Supplemental Figure 2A-B),** the copper binding mutant of full length PERK appeared kinase dead in comparison to its wild-type counterpart, both when analyzed by immunoblot or by ELISA for p-eIF2α. One of the two residues mutated in the copper binding mutant, histidine 935, is part of the HRD motif, which is well conserved among kinases. To ensure that the kinase dead phenotype was a result of the PERK CBM's inability to bind copper, and not a general kinase inactivating mutation, we cloned, purified, and assessed kinase activity of both wild-type and mutant versions of HRI, an eIF2α kinase family member of PERK. As seen in the alignment in **Figure 1C-D**, HRI retains a parallel HRD histidine at residue 440, but has an alanine at residue 497, compared with PERK's methionine at 991. As such a single mutation resulting in an alanine at residue 440 in HRI created an analogous change to that introduced into the kinase domain of the PERK CBM protein. This mutant protein showed lower but observable kinase activity compared to control under conditions of linear kinase activity **(Figure 2C, Supplemental Figure 2C-D**), confirming that while mutation of the HRD motif reduces kinase activity, the kinase dead phenotype of PERK CBM is due to its inability to bind copper. Furthermore, single mutation of the copper-binding coordinating residue methionine 991, which is not conserved in HRI and therefore not likely important for general eIF2 kinase activity, resulted in partial activity (**Figure 2B**), demonstrating the specific importance of this residue for copper-regulated kinase activity, and suggesting a dose-response relationship between PERK-copper binding and kinase activity.

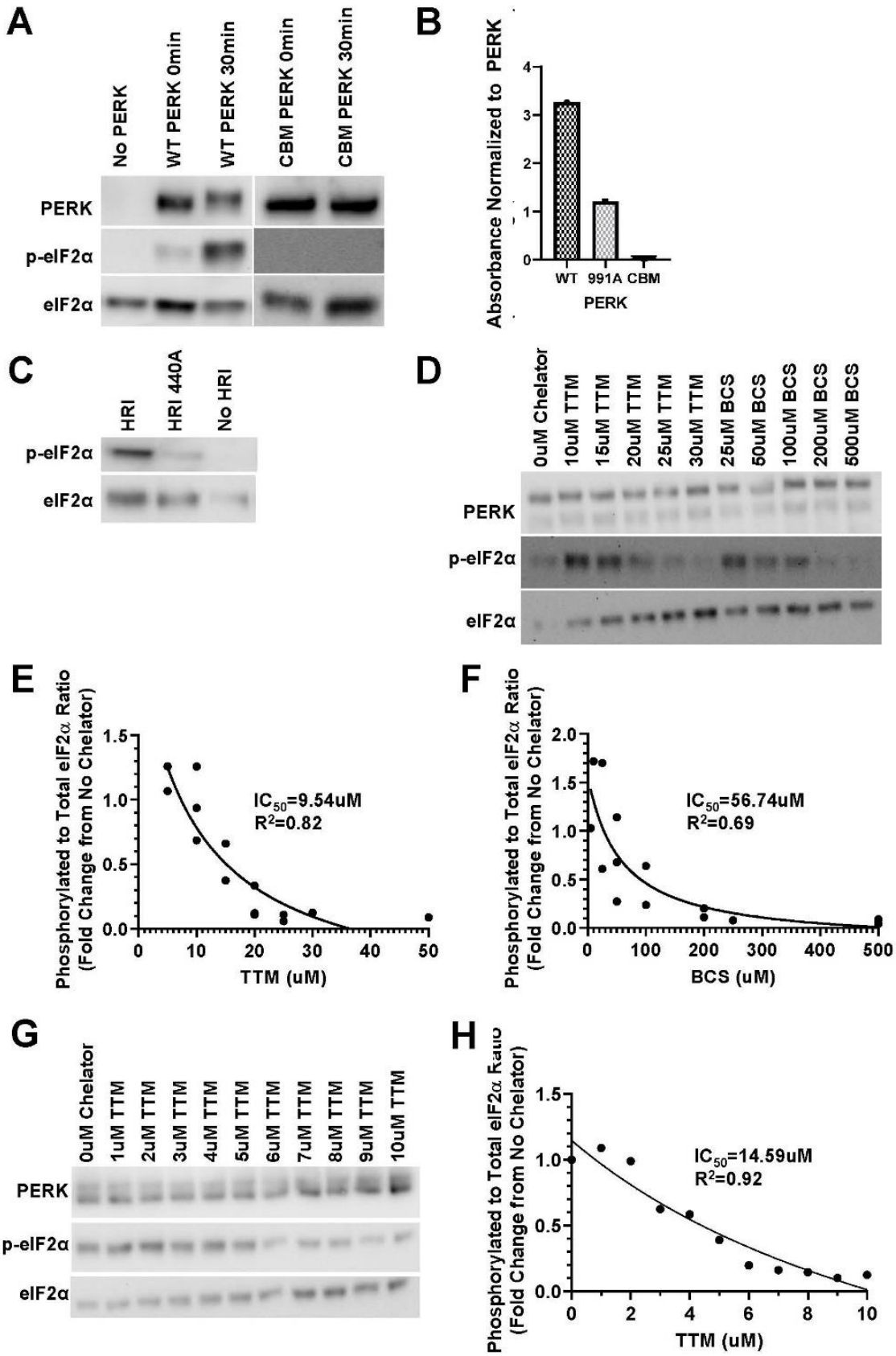
A
No PERK
WT PERK 0min
WT PERK 30min
CBM PERK 0min
CBM PERK 30min
PERK
p-eIF2α
eIF2α
B
Absorbance Normalized to PERK
WT
991A
CBM
PERK
C
HRI
HRI 440A
No HRI
p-eIF2α
eIF2α
D
0uM Chelator
10uM TTM
15uM TTM
20uM TTM
25uM TTM
30uM TTM
25uM BCS
50uM BCS
100uM BCS
200uM BCS
500uM BCS
PERK
p-eIF2α
eIF2α
E
Phosphorylated to Total eIF2α Ratio (Fold Change from No Chelator)
IC50=9.54uM
R2=0.82
TTM (uM)
F
Phosphorylated to Total eIF2α Ratio (Fold Change from No Chelator)
IC50=56.74uM
R2=0.69
BCS (uM)
G
0uM Chelator
1uM TTM
2uM TTM
3uM TTM
4uM TTM
5uM TTM
6uM TTM
7uM TTM
8uM TTM
9uM TTM
10uM TTM
PERK
p-eIF2α
eIF2α
H
Phosphorylated to Total eIF2α Ratio (Fold Change from No Chelator)
IC50=14.59uM
R2=0.92
TTM (uM)

Figure 2-Copper Binding is Required for PERK Kinase Activity
A) Representative western blot images, probed as indicated of PERK kinase assay reactions for indicated timepoints at 37°C.
B) ELISA quantification of p-eIF2α levels from 10 minute PERK kinase assay at 37°C (n=1).
C) Representative western blot images, probed as indicated of one hour HRI kinase assay reactions at 37°C.
D) Representative western blot images of ten minute reaction kinase assay at 37°C with varying concentrations of copper chelators, as indicated.
E) Quantification of n=3 variable replicates of the experiment shown in B; data points fit by least squares to a three-parameter dose-response inhibition curve. IC_{50} and R^2 of the fit curve indicated.
F) Quantification of n=3 variable replicates of the experiment shown in B; data points fit by least squares to a three-parameter dose-response inhibition curve. IC_{50} and R^2 of the fit curve indicated.
G) Western blot images, probed as indicated, of five minute kinase reaction at 37°C with varying concentrations of TTM, as indicated.
H) Quantification of n=1 of the experiment shown in E; data points fit by least squares to a three-parameter dose-response inhibition curve. IC_{50} and R^2 of the fit curve indicated.
CBM=Copper Binding Mutant; TTM=Tetrathiolmolybdate; BCS=Bathocuproine Disulfonic Acid.

PERK-copper binding was found to regulate PERK in a dose-dependent manner by several additional measures. In addition, two copper specific chelators, bathocuproine disulfonic acid (BCS) and TTM, were found to inhibit PERK in *in vitro* kinase assays in a dose-dependent fashion, such that p-eIF2α levels as a read out for PERK activity could be well fitted to an inhibition curve against increasing concentrations of chelator (**Figure 2D-F**). Similar trends were seen with the GST-tagged PERK kinase domain and TTM (**Figure 2G-H, Supplemental Figure 2E-F**). Overall these results indicate that PERK requires copper binding for kinase activity, unlike another eIF2α kinase family member, HRI.

2.3 Copper manipulation can modulate PERK activity in cells

We next sought to translate our *in vitro* findings into the cellular context by determining whether manipulating intracellular copper, either genetically or pharmacologically, affected PERK activity as measured by eIF2α phosphorylation. MEFs were pretreated with copper chelators BCS and TTM, followed by pharmacological PERK inducers, PERK activator (PA) and thapsigargin (Tg), respectively. In these experiments, CCS, the stability of which has an inverse relationship with copper, was used as a readout for effective copper chelation (Bertinato and

L'Abbe, 2003; Caruano-Yzermans et al., 2006). As seen in **Figure 3**, copper chelation significantly inhibited PERK phosphorylation of eIF2a in response to treatment with thapsigargin **(Fig. 3A-B**) or PERK activator **(Fig. 3E-F**). The same was true in rat cortical cultures (data not shown). In the absence of PERK however, neither thapsigargin nor PERK activator significantly induced eIF2a phosphorylation and chelation of copper had no significant effect (**Figure 3A-B, E-F**). Furthermore, when salubrinal (Sal), an inhibitor of eIF2α dephosphorylation, was used to induce eIF2α phosphorylation in a non-PERK-dependent fashion, neither chelator had a significant effect, although salubrinal also failed to be a significant inducer of eIF2α phosphorylation (**Figure 3C-D, G-H**). These results indicate that copper chelation can be used to reduce PERK-mediated eIF2α phosphorylation upon PERK induction.

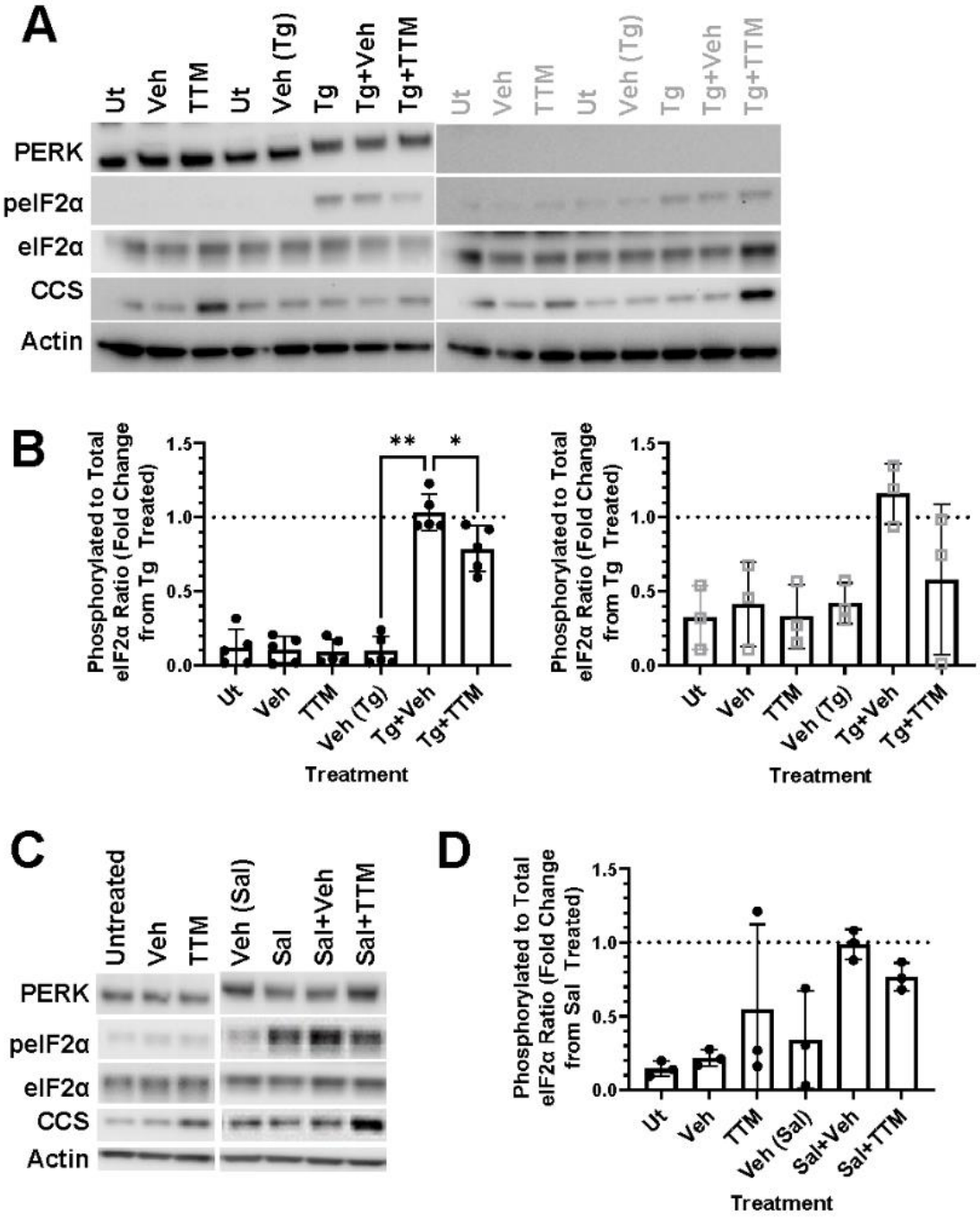
A
Ut
Veh
TTM
Ut
Veh (Tg)
Tg
Tg+Veh
Tg+TTM
PERK
peIF2α
eIF2α
CCS
Actin
B
Phosphorylated to Total eIF2α Ratio (Fold Change from Tg Treated)
1.5
1.0
0.5
0.0
**
*
Treatment
C
Untreated
Veh
TTM
Veh (Sal)
Sal
Sal+Veh
Sal+TTM
D
Phosphorylated to Total eIF2α Ratio (Fold Change from Sal Treated)

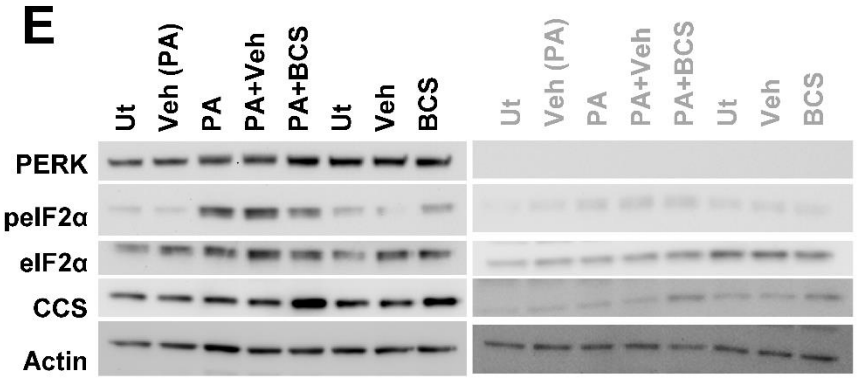
E
Ut
Veh (PA)
PA
PA+Veh
PA+BCS
Ut
Veh
BCS
PERK
peIF2α
eIF2α
CCS
Actin

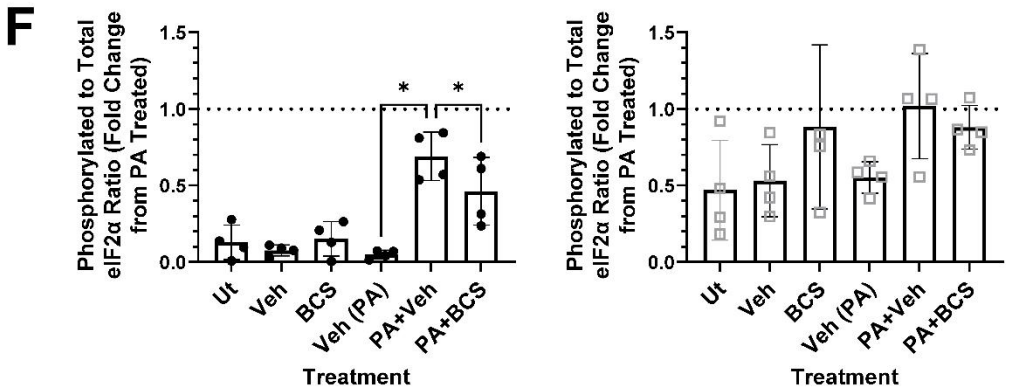
F
Phosphorylated to Total eIF2α Ratio (Fold Change from PA Treated)
1.5
1.0
0.5
0.0
*
*
Ut
Veh
BCS
Veh (PA)
PA+Veh
PA+BCS
Treatment

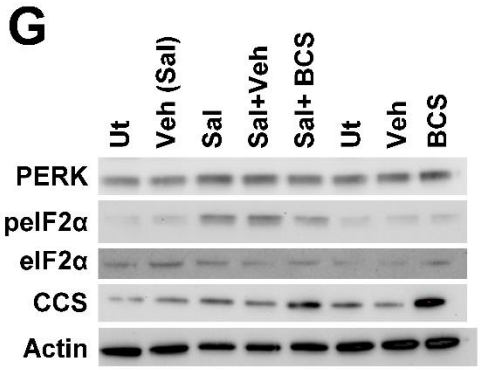
G
Ut
Veh (Sal)
Sal
Sal+Veh
Sal+ BCS
Ut
Veh
BCS
PERK
peIF2α
eIF2α
CCS
Actin

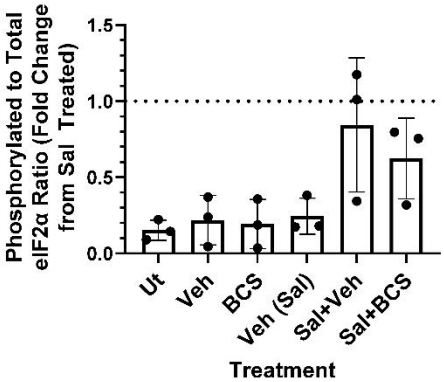
H
Phosphorylated to Total eIF2α Ratio (Fold Change from Sal Treated)
1.5
1.0
0.5
0.0
Ut
Veh
BCS
Veh (Sal)
Sal+Veh
Sal+BCS
Treatment

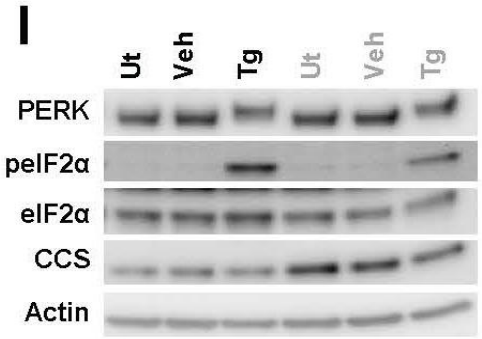
I
Ut
Veh
Tg
Ut
Veh
Tg
PERK
peIF2α
eIF2α
CCS
Actin

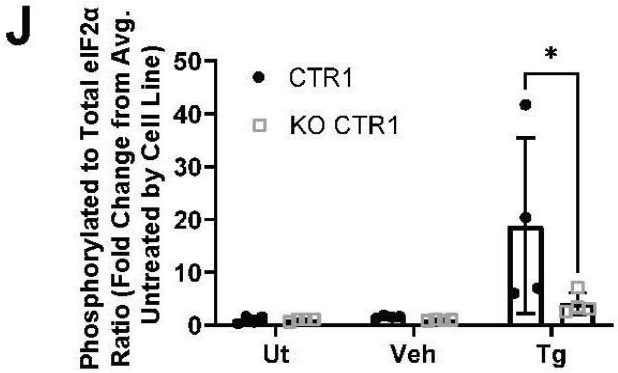
J
Phosphorylated to Total eIF2α Ratio (Fold Change from Avg. Untreated by Cell Line)
50
40
30
20
10
0
CTR1
KO CTR1
*
Ut
Veh
Tg

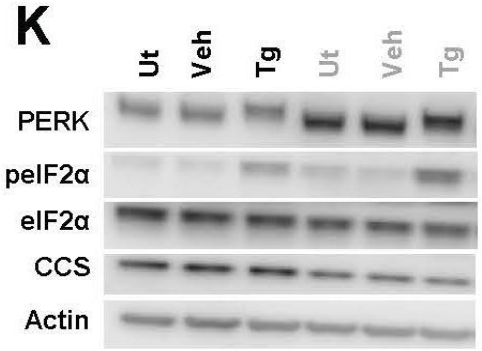
K
Ut
Veh
Tg
Ut
Veh
Tg
PERK
peIF2α
eIF2α
CCS
Actin

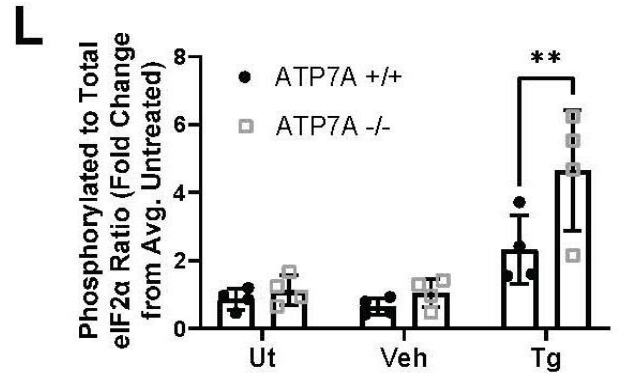
L
Phosphorylated to Total eIF2α Ratio (Fold Change from Avg. Untreated)
8
6
4
2
0
ATP7A +/+
ATP7A -/-
**
Ut
Veh
Tg

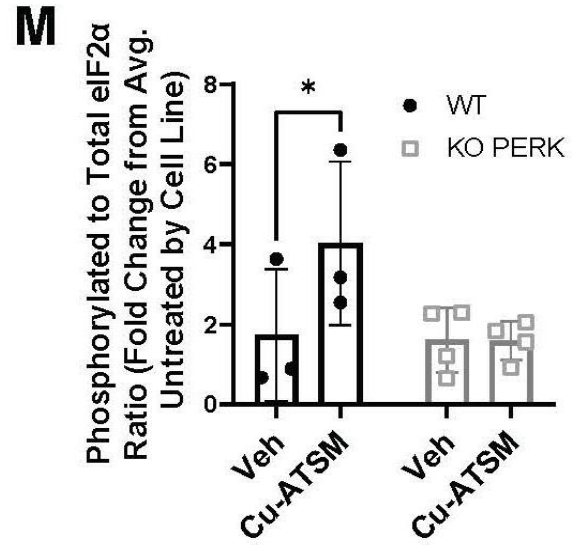
M
Phosphorylated to Total eIF2α Ratio (Fold Change from Avg. Untreated by Cell Line)
8
6
4
2
0
WT
KO PERK
*
Veh
Cu-ATSM
Veh
Cu-ATSM

Figure 3-Copper Manipulation can Modulate PERK activity in the Cell
A) Representative western blot images, probed as indicated, of WT and KO PERK (gray) MEF whole cell lysates from cells treated with 15uM TTM for 24 hours and 300nM Tg for 2hrs.
B) Quantification of n=3-4 replicates of the experiments in A. One-way repeated measures ANOVA returned significant effect of treatment for WT. $p<0.0001$. Holm-Sidak's multiple comparison test: *$p<0.05$; **$p<0.01$. One-way repeated measures ANOVA did not return significance for KO PERK. $p=0.185$.
C) Representative western blot images, probed as indicated, of MEF whole cell lysates from cells treated with 15uM TTM for 24 hours and 50uM Sal for 24hrs.
D) Quantification of n=3 replicates of the experiment in C. One-way repeated measures ANOVA did not return significance. $p=0.13$.
E) Representative western blot images, probed as indicated, of WT and KO PERK (gray) MEF whole cell lysates from cells treated with 500uM BCS for 24 hours and 10uM PA for 1 hour.
F) Quantification of n=4 replicates of the experiment in E. One-way repeated measures ANOVA returned significant effect of treatment for WT. $p=0.0046$. Holm-Sidak's multiple comparison test: *$p<0.05$. One-way repeated measures ANOVA did not return significance for KO PERK. $p=0.163$.
G) Representative western blot images, probed as indicated, of MEF whole cell lysates from cells treated with 500uM BCS for 24 hours and 50uM Sal for 24 hours.
H) Quantification of n=3 replicates of the experiment in G. One-way repeated measures ANOVA did not return significance. $p=0.054$.
I) Representative western blot images, probed as indicated, of CTR1 and KO CTR1 (gray) whole cell lysates from cells treated with 300nM Tg for 2 hours.
J) Quantification of n=4 replicates of the experiment in I. Two-way repeated measures ANOVA returned treatment as a significant factor. $p=0.014$. Sidak's was used for multiple comparisons. *$p<0.05$.
K) Representative western blot images, probed as indicated, of ATP7A +/+ and ATP7A -/- (gray) whole cell lysates from cells treated with 300nM Tg for 2 hours.
L) Quantification of n=4 replicates of the experiment in K. Two-way repeated measures ANOVA returned treatment as a significant factor, $p<0.0001$, as well as a significant interaction between treatment and genotype, $p=0.023$. Sidak's test was used for multiple comparisons. **$p<0.01$.
M) Quantification of n=3 replicates of experiment where MEFs were treated with 100uM Cu-ATSM for 1hr before being harvested and whole cell lysates immunoblotted for peIF2α, eIF2α, Actin and PERK. Two-way repeated measures ANOVA returned treatment and genotype interaction as a significant factor, $p<0.05$. Sidak's test was used for multiple comparisons. *$p<0.05$.
Tg=thapsigargin; PA=PERK Activator; Sal=Salubrinal; TTM=Tetrathiolmolybdate; BCS=Bathocuproine Disulfonic Acid; CCS=copper chaperone for SOD1; KO=knockout; MEF=mouse embryonic fibroblast.

In an additional set of experiments MEFs either not expressing (KO CTR1) or overexpressing copper transporter 1 (CTR1) were compared for their response to thapsigargin treatment. Given that CTR1 is the cell's main copper importer, KO CTR1 cells were expected to have lower copper content, as confirmed by ICP-MS (**Supplemental Figure 3B**) (Magistrato et al., 2019). In following, KO CTR1 MEFs were shown to have a significantly decreased response to thapsigargin, comparable to untreated, after adjusting for baseline differences in p-eIF2α, which were also significantly different (**Figure 3I-J, Supplemental 3C**), demonstrating that copper-depleted cells have a stressed basal state and impaired activation of the PERK upon ER stress. In parallel, a pair of MEFs with the ATP7A gene either floxed (ATP7A +/+) or excised

(ATP7A -/-) were also examined for their response to thapsigargin. Given that ATP7A is a copper exporter, its deletion resulted in higher cellular copper content, as measured by ICP-MS (**Supplemental Figure 3B**) (Magistrato et al., 2019). In the ATP7A -/- cells, significantly enhanced phosphorylation of eIF2α upon thapsigargin treatment was observed compared to ATP7A +/+ cells (**Figure 3K-L**), suggesting that, in the cell, PERK activity in response to ER stress may be bi-directionally modulated by intracellular copper availability, and thus, that copper may be an endogenous signaling regulator of PERK. Furthermore treatment with the copper ionophore Cu-ATSM, was sufficient to induce eIF2α phosphorylation in a PERK dependent manner in the absence of stress (**Figure 3M**), suggesting that copper is not only necessary, but sufficient for PERK induction.

2.4 Copper mediated regulation of PERK can impact ER stress tolerance

Given the ability to bi-directionally modulate PERK-mediated eIF2α phosphorylation by manipulation of cellular copper availability, as demonstrated in **Figure 3,** we next examined the effect of such changes, specifically evaluating changes in protein folding machinery and apoptosis sensitization and induction down-stream from PERK induction. These experiments sought to determine whether such changes constituted altered ER stress tolerance, as this has previously been shown to be a PERK dependent phenotype (Berlanga et al., 2006; Bi et al., 2005; Boyce et al., 2005; Gupta et al., 2012; Harding et al., 2000; Harding et al., 2003; Liu et al., 2015; Lu et al., 2004; Tan et al., 2001; Walter and Ron, 2011; Wek et al., 2006).

To do this we first established conditions where KO PERK cells exhibited greater lactose dehydrogenase (LDH) release than WT cells, indicative of cytotoxicity, in response to 20 hour treatments of thapsigargin and tunicamycin. Thapsigargin inhibits the ER calcium pump, SERCA, and dysregulates ER calcium homeostasis, and therefore chaperone activity. Tunicamycin (Tm) causes protein misfolding by inhibiting N-linked protein glycosylation. Using this experimental paradigm, in line with previous findings, stress inducers, thapsigargin and

tunicamycin. were sufficient to induce cytotoxicity in both WT and PERK KO MEFs, but KO PERK MEFs released more LDH, indicating a deficit in ER stress tolerance (**Figure 4A-B**). As seen in **Figure 4C-D**, a parallel set of experiments with ATP7A +/+ and ATP7A -/- MEFs demonstrated that the ATP7A -/- MEFs released less LDH in response to ER stress inducers that ATP7A +/+ MEFs, suggesting these copper replete cells have enhanced ER stress tolerance.

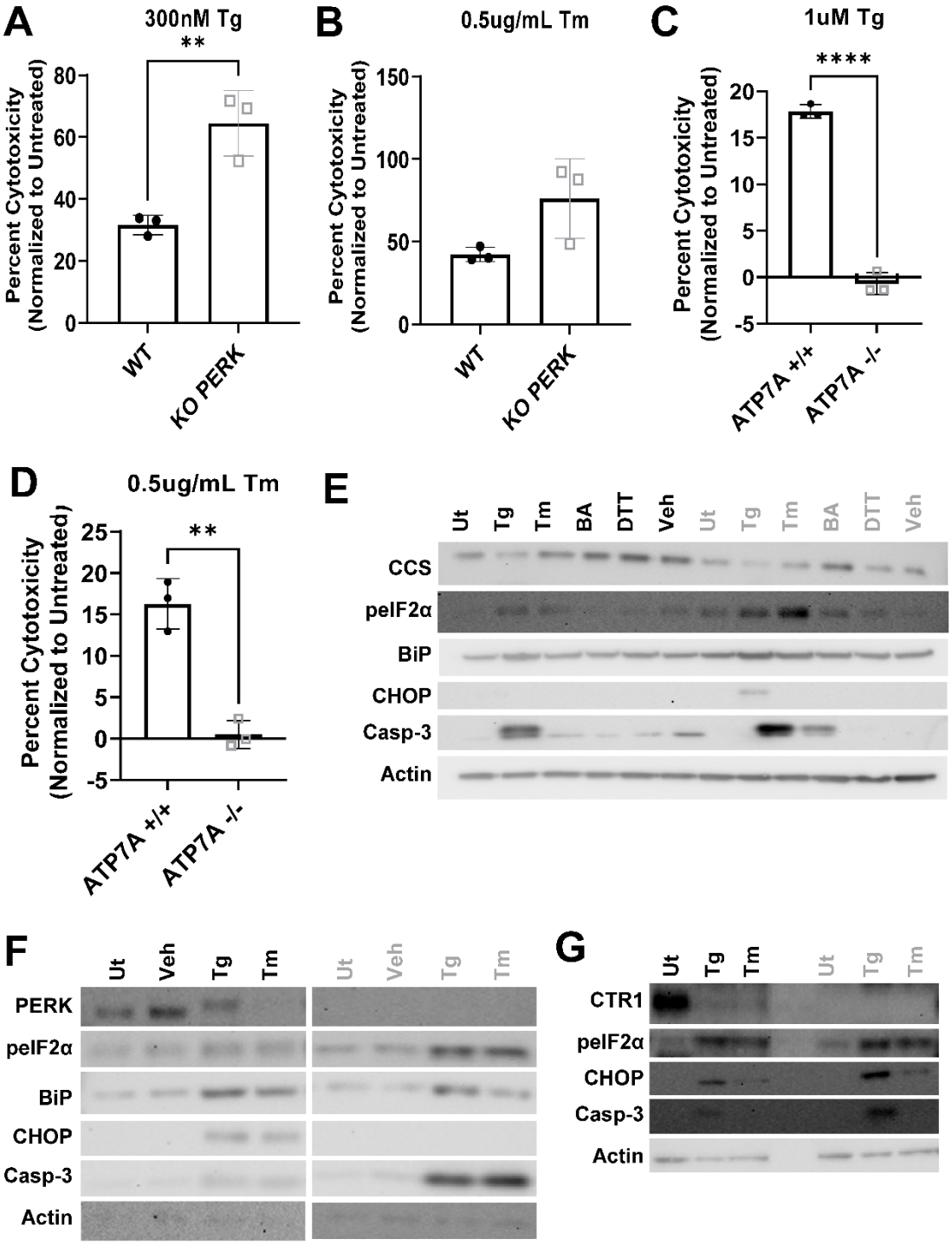
A
300nM Tg
**
Percent Cytotoxicity (Normalized to Untreated)
80
60
40
20
0
WT
KO PERK
B
0.5ug/mL Tm
150
100
50
0
WT
KO PERK
C
1uM Tg
****
20
15
10
5
0
-5
ATP7A +/+
ATP7A -/-
D
0.5ug/mL Tm
**
25
20
15
10
5
0
-5
ATP7A +/+
ATP7A -/-
E
Ut
Tg
Tm
BA
DTT
Veh
CCS
peIF2α
BiP
CHOP
Casp-3
Actin
F
Ut
Veh
Tg
Tm
PERK
peIF2α
BiP
CHOP
Casp-3
Actin
G
Ut
Tg
Tm
CTR1
peIF2α
CHOP
Casp-3
Actin

Figure 4-Copper Manipulation can Modulate ER Stress Tolerance
A) LDH Assay results quantifying LDH release as a measure of cytotoxicity from WT (black) and KO PERK (grey) MEFs treated with 300nM Tg for 20 hours. n=3.
B) LDH Assay results quantifying LDH release as a measure of cytotoxicity from WT (black) and KO PERK MEFs (grey) treated with 0.5ug/mL Tm for 20 hours. n=3.
C) LDH Assay results quantifying LDH release as a measure of cytotoxicity from ATP7A +/+ (black) and ATP7A -/- (grey) MEFs treated with 1uM Tg for 20 hours. n=3.
D) LDH Assay results quantifying LDH release as a measure of cytotoxicity from ATP7A +/+ (black) and ATP7A -/- (grey) MEFs treated with 0.5ug/mL Tm for 20 hours. n=3.
E) Representative western blot images of protein lysates from ATP7A +/+ (black) and ATP7A -/- (grey) MEFs treated with 300nM Tg or 0.5ug/mL Tm for 20 hours. n=3.
F) Western blot images of protein lysates from WT (black) and KO PERK (gray) whole cell MEF lysates, treated for 20hrs with 300nM Tg or 0.5ug/mL Tm for 20 hours. n=1.
G) Representative western blot images of protein lysates from CTR1 (black) and KO CTR1 (grey) MEFs treated with 300nM Tg or 0.5ug/mL Tm for 20 hours. n=3.
Tg=thapsigargin; Tm=tunicamycin; Casp-3=Cleaved Caspase-3; KO=knockout; MEF=mouse embryonic fibroblast; LDH=lactose dehydrogenase; BA=Brefedlin A.

Western blot analysis of parallel experiments showed that the higher levels of PERK signaling, including elevated levels of p-eIF2α, BiP, CHOP, and Cleaved Caspase 3, in the stress resistant ATP7A -/- cells, as compared to ATP7A +/+ cells (**Figure 4E**). In contrast, WT MEFs had higher BiP and CHOP induction as compared to KO PERK MEFs, but lower eIF2α phosphorylation and Caspase 3 cleavage (**Figure 4F**). Similar to ATP7A -/- cells, upregulation of PERK signaling was also seen in KO CTR1 MEFs, relative to CTR1 MEFs, under chronic stress conditions (**Figure 4G**). The relationship of these signaling events with ER stress tolerance is yet to be established.

3. Discussion

In the above series of studies, we have shown that PERK binds copper (**Figure 1**), that this binding is required for kinase activity (**Figure 2**), that this interaction can be used to modulate PERK induction in cells (**Figure 3**), and that such modulation may affect down-stream PERK cell fate outcomes via altered protein homeostasis signaling (**Figure 4)**. All together these results demonstrate that copper binding is a physiologic modulator of PERK activity that has broad implications for PERK signaling, its regulation, and its downstream effects on proteostasis and other interconnected cellular processes.

In Figure 1 PERK was shown to interact with copper under both cellular and in *vitro* conditions. *In vitro* it was also shown to have some ability to bind zinc. This interaction was weak though, as indicated by its ability to be perturbed by a non-competitive wash, suggesting that it may be an artifact of the *in vitro* environment and not a specific interaction. However dual specificity zinc and copper binding pockets have been characterized in other proteins, such as SOD1, and this study does not eliminate that possibility. We also identified residues that play a role in PERK's coordination of copper, Histidine 935 and Methionine 991, and confirmed by ICP-MS that mutation of these residues results in loss of copper binding. Intriguingly, our ICP-MS results also indicated that wild-type PERK existed in the cell in a partially bound state, the stoichiometric ratio of which could be increased via incubation with glutathione complexed copper. The difference between the two states is likely a result of occupancy, and not multiple binding sites. The binding site and 1:2 ratio implies that copper may be coordinated by PERK dimers.

These studies leaves several parameters of the PERK-copper binding relationship uncharacterized, which would be of interest in future studies. Such parameters include verification of the stoichiometry of PERK-copper binding, the affinity of this interaction, and the redox state of copper when bound. The cellular environment of the cytosol, and the conditions required for PERK-copper interaction in our *in vitro* studies suggest that PERK binds copper it its cuprous (I) state, and that, unlike other recently characterized copper binding enzymes, it is unable to bind or reduce cupric (II) copper (Attar et al., 2020; Grasso et al., 2020; Grasso et al., 2021). However, further biophysical studies utilizing electron paramagnetic resonance (EPR), X-ray absorption spectroscopy (XAS), and extra X-ray absorption fine structure (EXFAS) would be required to confirm these hypotheses by absence of a detectable copper II bound state.

In Figure 2 we demonstrated that copper-binding is absolutely required for PERK kinase activity. Lacking a structure, any hypotheses as to the mechanism of copper mediated PERK-activity remain purely hypothetical. Still several possibilities in agreement with available

literature are worthy of note. The likely utilization of the HRD motif histidine in coordination of copper, as well as the absolute requirement of copper for kinase activity, be it auto-phosphorylation or substrate phosphorylation, suggests a direct catalytic activity on the kinase reaction, plausibly via stabilization or coordination of the flexible catalytic loop. Intriguingly Methionine 991 is located at the C-terminal end of the activating loop, adjacent to residues that were unable to be resolved in the previously published PERK kinase domain crystal structure, with the authors inferring that the activation loop was still partially disordered under the crystallization conditions (Cui et al., 2011). Parallel to this, MEK residues following Methionine 230, were structured in its crystal structure, but not the copper-bound one, suggesting that copper binding might stabilize the end of the activation loop at the expense of the following residues (Grasso et al., 2020). An additional consideration is that PERK, MEK and ULK contain a disordered insert loop at the C-terminal end of the N-lobe, prior to the interlobe/hinge region (Chaikuad et al., 2019; Cui et al., 2011; Fischmann et al., 2009; Grasso et al., 2020). Although relatively distanced from the binding site, it is possible that copper binding alters the conformation and/or stabilizes this region, particularly as it is known to be disordered. Another possibility comes from a recent study demonstrating that PERK activity can be enhanced by S-nitrosylation (Nakato, 2015). This type of post-translational modification requires an electron donor and copper is known to act in this role in its addition to other proteins. The fact the PERK bound copper can be quantified by ICP-MS suggests a different, or at least additional, use of copper than such a transitional activity, however.

In Figure 3 we proved that we could modulate PERK activity in the cell by manipulating cellular copper, and in Figure 4 we showed that these signaling differences translated to altered ER stress tolerance. Specifically, while PERK down-stream apoptotic markers are up in stress resistant, copper replete ATP7A -/- cells, so were all PERK down-stream signals, such as the proteostatic chaperone BiP. In line with this, at the 20 hour time point we see greater eIF2α phosphorylation in KO PERK cells as compared with WT cells, suggesting that stress has

accumulated/not been resolved in the former, where PERK activity is ablated. Stronger basal level and BiP induction in WT and ATP7A -/- cells may outweigh CHOP signaling, allowing re-establishment of protein homeostasis and mitigating PERK induced cell-death.

While the findings presented here were novel, retrospective analysis of the literature provides surprising amount of support for copper regulation of PERK and its implications. Most notably, UPR induction, specifically PERK signaling, was recently documented in a mouse model of Wilson's Disease, where copper iss in excess (Chen et al., 2018). Furthermore, this PERK signaling was shown to be cytotoxic, contributing to cerebrovascular injury and apoptosis, and to be alleviated by treatment with the copper chelator DPA, in combination with traditional Chinese medicine (TCM) agent GanDouLing. These findings support the notion that altered copper homeostasis can result in aberrant PERK signaling. In the same vein, another study documented that PDTC-complexed copper exposure induced apoptosis in lung epithelial cells via ER stress, as well as mitochondria stress (Chen et al., 2010). In another study, drug resistant renal cell carcinoma cells, were shown to be effectively targeted for apoptosis, again via ER-stress and mitochondrial pathways, by cuprous oxide nanoparticles (CONPs), without systematic toxicity (Yang et al., 2017). Notably, the study highlighted apoptosis induction by ER-stress mediated mechanisms, with observations of strong UPR induction and ER swelling. The study also noted the accumulation of copper in the cytosol, and the down regulation of copper regulatory chaperones upon CONPs treatment, with many of the effects appearing to be mediated by such down regulation (Yang et al., 2017). Induction of the cytotoxic UPR, by both CONPs and knockout of CCS and ATOX1 suggest not only possible copper mediated PERK activity, but also a possible role for copper loading of PERK under basal settings, such as would explain the ER stress phenotype upon copper delivery chaperone knockout.

In sum, copper regulation of PERK, as shown here, paves the way to many future studies, both thoroughly delineating the biochemical and cellular mechanisms of this regulation,

and investigating how novel recognition of this regulation both explains and further crosses the interplay of ER stress and other signaling responses to affect cellular outcomes.

4. Materials and Methods

Plasmids

PERK cDNA constructs were cloned from pTCN background gift constructs from Gerard Schellenberg. The full length cDNA and kinase domain sequences were subcloned into a pcDNA3.1 C-terminal FLAG-tagged vector, with or without an N-terminal HA-tag. HRI cDNA in the pMD18 vector background was purchased from SinoBiological and subcloned into the same. Cloning was done by Gibson assembly utilizing NEB HiFi Assembly Master Mix. Mutations of the copper binding site were inserted using the Agilent Site Directed Mutagenesis kit. All construct sequences were verified with sequencing by the University of Pennsylvania, Department of Genetics Sequencing Core.

DNA Purification

DNA was produced by transformation of OneShot competent *E. coli* according by manufacturer instructions and grown in Luria Broth with Carbenicllin. DNA was purified using the ThermoFisher HiPure Purification kit according to manufacturer instructions. DNA concentrations were quantified on a Nanodrop 2000c.

Protein Expression and Purification

Protein construct expression was performed by transfection into ThermoFisher 293F cells according to the product manual, utilizing FreeStyle MAX transfection reagent diluted in OptiPRO SFM and 312.5ug of DNA per 250mL of culture. Expression proceeded for 2-3 days before harvesting by centrifugation for 5 minutes at 3,000g at 4°C. The pellet was resuspended with 1mL lysis buffer/25mL culture, composed of 25mM Tris-HCl, 150mM NaCl, 1mM EDTA, 1%

NP-40, and 5% glycerol supplemented with Halt Phosphatase and Protease Cocktail Inhibitor Cocktail, mammalian protease inhibitor cocktail without chelators, and sodium orthovanadate, added immediately before use. Complete lysis was ensured by vortexing, homogenization, and sonication for 15 seconds, followed by 15 seconds of rest for 3 cycles, all on ice. Lysates were centrifuged for 25 minutes at 30,000g, 4°C to pellet cellular debris. The supernatant was collected and added to a spin column containing 1mL packed, rinsed, and equilibrated anti-FLAG resin from Thermofisher. The lysate was incubated with the resin with agitation for 2 hours at 4°C. The column was then centrifuged 2 minutes at 1000g, 4°C, and the full-through collected for purification analysis. The resin was washed 4 times with 5 mL buffer, first with lysis buffer, then with lysis buffer + 300mM NaCl, incubated for 10 minutes at 4°C with agitation, twice, then with lysis buffer again. Washes were incubated for 10 min at 4°C with agitation. The protein was eluted using 2mL 1.25mg/mL 3X Flag Peptide from Thermofisher in lysis buffer. Elutant was cleaned up by and concentrated using Amicon 10kda MWCO ultrafiltration columns, and repurified with anti-FLAG resin as necessary. Protein concentration measured was by Bradford Assay. Purity of final product was assessed by western blot and Coomassie staining.

IMAC pull-down

For IMAC pull-down experiments Bio-Rad IMAC resin was rinsed and charged with 200mM of different metal ions in Tris-HCL. Excess metal was then removed by 5 washes and the charged resin incubated with 100ug cell lysate or 100ng GST-PERK for 2 hours at 4C. FT was collected and bound protein was eluted with titrations of binding buffer (Tris HCL, 100mM NaCL) plus varying concentrations of imidazole. Flow-through, wash, and elution samples were analyzed by western blot.

ICP-MS

Samples were submitted to the PADLS toxicology lab at the New Bolton Center for the University of Pennsylvania, School of Veterinary Medicine for processing.

Kinase Assay

Kinase assays were prepared utilizing CST Kinase Buffer and 100uM ATP. For kinase assays with GST-tagged PERK Kinase domain, 20ng GST-PERK was combined with 7.3ng His-eIF2α in a 50uL reaction for a 4.2nM:4.2nM substrate:enzyme molar ratio. For kinase assays with FLAG tagged full-length PERK, 100ng was combined with 7.3ng His-eIF2α in a 50uL reaction for a 4.2nM:16.8nM molar ratio. After incubation, 50uL reactions were terminated with the addition of 4X NuPAGE LDS, 10X NuPAGE Sample Reducing Agent, and water up to 80uL. 20uL of the final reaction mixture was used for blotting. For kinase reactions with FLAG-tagged HRI, 630ng was combined with 500ng His-eIF2α in a 10uL reaction for a 1.4uM:875nM molar ratio. After incubation these reactions were terminated with 4X LDS, 10X Reducing Buffer, and H2O up to 270uL. 1uL of this solution was used for preparation of western blot samples, made up to 20uL with 4X LDS, 10X Reducing Buffer, and H2O.

Cell culture

WT and KO PERK MEFs, immortalized with SV40, were the kind gift of Dr. Koumenis. CTR1 KO and wild-type CTR1 MEFs, and ATP7A Floxed +/+ and Cre treated -/- lines were the generous gift of Dr. Donita Brady. MEFs were cultured in DMEM with GlutaMAX and 10% FBS. According to experiment cells were treated with Thapsigragin (Torcis), PERK Activator (Millipore), Tunicamycin (Torcis), Brefedlin A (Torcis), DTT (Sigma), Cu-ATSM (Cayman Chemical), Salubrinal (Sigma), TTM (Sigma), and BCS (Sigma) at various time points and doses as indicated in the results section. Whole cell lysates were harvested utilizing NP-40 buffer and protein was quantified by Bradford Assay using Biorad reagent.

Gel Electrophoresis

Samples were prepped by combination with 4X LDS (Invitrogen) and 10X Reducing Buffer (Invitrogen) and heated for 10min at 70°C. Samples were loaded into 4-12% Bis-Tris gels (Invitrogen) and ran out at 130V in MOPS running buffer.

Western Blot

Gels for western blotting were transferred to PVDF membrane for 2.5 hours to overnight at 4°C in Thermofisher Transfer buffer at 30V. Blots were then rinsed with Tris-buffered saline (TBS) and TBS with 0.1% Tween-20 (TBS-t) before being blocked 1 hour at room temperature in TBS-T + 5% BSA. Blot were incubated in primary antibody diluted in blocking buffer overnight. Primary antibodies and dilutions used were: 1:1000 Rabbit anit Ser 51 peIF2α (CST), 1:1000 Rabbit anti D9G8 peIF2α (CST), 1:1000 Mouse anti eIF2α (CST), 1:1000 Rabbit anti PERK (CST), 1:1000 Rabbit anti FLAG (CST), 1:40,0000 Mouse anti B-Actin (CST), 1:1000 Rabbit anti Calcineurin (CST), 1:1000 Mouse anti CHOP (CST), 1:1000 Rabbit anti Cleaved Caspase 3 (CST), 1:1000 Rabbit anti CTR1 from (CST), 1:1000 Rabbit anti CCS from (Abcam), 1:1000 Rabbit anti ATP7A (Sigma), 1:1000 Rabbit anti HRI (Sigma) and 1:2000 Mouse anti BiP (BD). Blot were washed with TBS-T and incubated with 1:2000 Goat anti Rabbit or 1:5000 Goat anti Mouse HRP conjugated antibodies (Jackson) diluted in blocking buffer for 30 minutes at room temperature. Blots were washed an additional three time with TBS-T and one time with TBS before 3 minute exposure with ECL HRP substrate (Millipore) and imaged on a BioRad ChemiDoc system. Images were quantified using ImageLab software.

LDH Assay

Roche LDH Cytotoxicity Assay was optimized and performed according to kit manufacturer instructions (#11644793001). LDH activity was quantified using a ThermoFisher Multiskan™ FC Microplate Photometer at 492nm.

Statistical analysis

All statistical analyses were performed using GraphPAD PRISM software.

5. Acknowledgements

This work was funded by NIH/NIMH R01MH109382, NIH T32GM008275 Structural Biology and Molecular Biophysics Training Grant, and the University of Pennsylvania BGS Training Grant.

6. Supplemental Figures

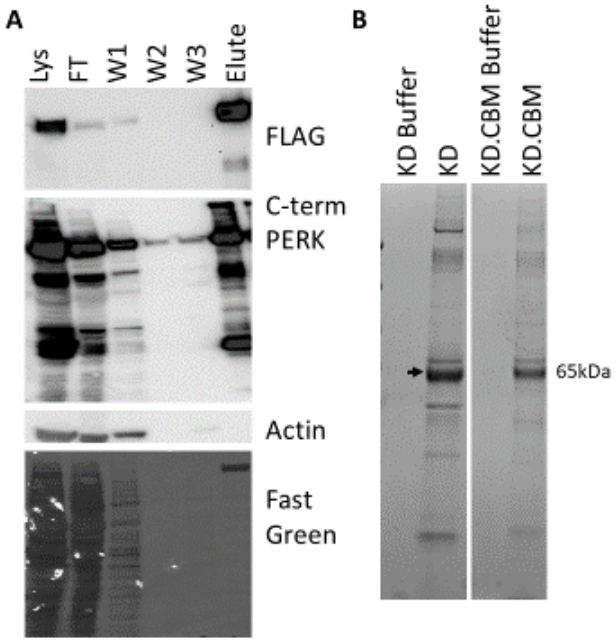

C

Sample	PPM
KD Buffer	0.0707
KD	0.138
KD.CBM Buffer	0.104
KD. CBM	0.0716
Cu Charged KD Buffer	0.440
Cu Charged KD	0.0783

Supplemental Figure 1-PERK Protein Purification
A) Western blot images, probed as indicated of representative PERK protein purification process. Lys=lysate; FT=Flow though; W=Wash.
B) Coomassie stained gel of purified PERK kinase domain (KD) protein samples submitted for ICP-MS. Target band indicated by arrow in relation to molecular weight marker. CBM=Copper Binding Mutant.
C) Table of raw results from ICP-MS analysis. PPM=Parts per million.

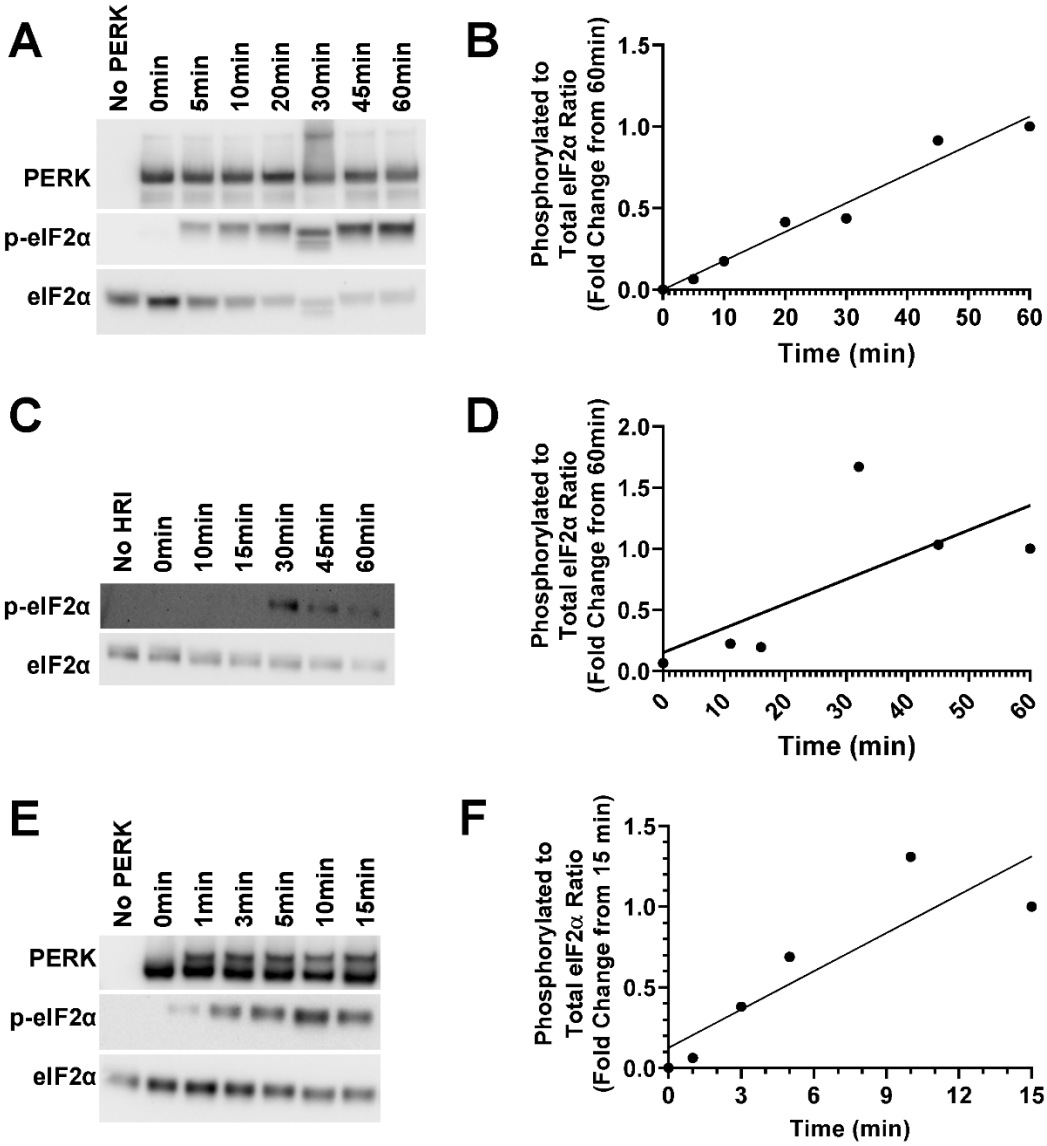

Supplemental Figure 2-Kinase Assay Conditions

A) Western blot images, probed as indicated, of kinase assay reaction with 16.8nM PERK-FLAG and 4.2nM His-eIF2α, incubated at 4°C and terminated at the indicated time points.

B) Quantification of experiment in A fit to a simple linear regression. R^2=0.967. Slope in non-zero, p<0.0001.

C) Western blot images, probed as indicated, of kinase assay reaction with 875nM HRI-FLAG and 1.4μM His-eIF2α, incubated at 37°C and terminated at the indicated time points.

D) Quantification of experiment in C with attempted fit to a simple linear regression. R^2=0.506. Slope is not significantly non-zero, p=0.1132.

E) Western blot images, probed as indicated, of kinase assay reaction with 4.2nM GST-PERK kinase domain and 4.2nM His-eIF2α, incubated at 25°C and terminated at the indicated time points.

F) Quantification of experiment in E fit to a simple linear regression. R^2=0.768. Slope in non-zero, p=0.022.

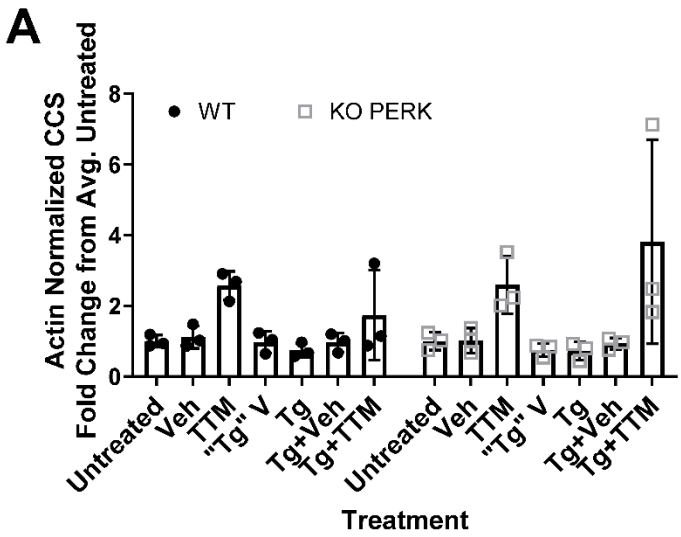

B

Sample	PPM
WCLB	0.376
ATP7A +/+	0.438
ATP7A -/-	0.504
CTR1	0.234
KO CTR1	0.0875

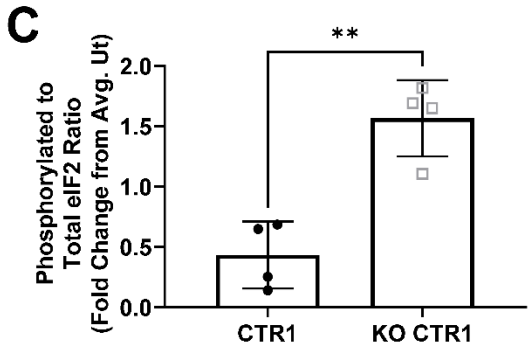

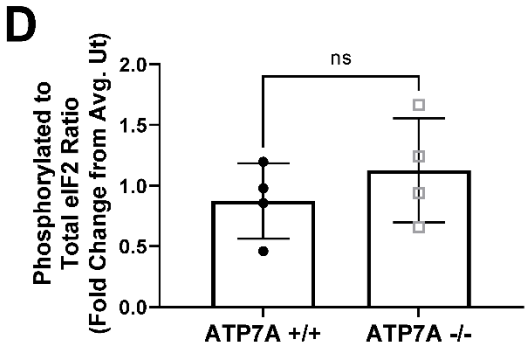

Supplemental Figure 3-Manipulation of Copper Availability in MEFs
A) Quantification of CCS from western blot images from 3 replicates of experiment shown in Figure 2.3A. WT and KO PERK MEFs treated with 15uM TTM for 24 hours and 300nM Tg for 2 hours.
B) ICP-MS results indicating copper content of different cell lines.
C) Quantification of untreated p-eIF2α from western blot images of n=4 replicates for the experiment shown in Figure 2.3I-J. Two-way t-test. **$p<0.01$.
D) Quantification of untreated p-eIF2α from western blot images of n=4 replicates for the experiment shown in Figure 2.3K-L. Two-way t-test. $p>0.05$.
Tg=thapsigargin; WT=wild-type; KO=knock-out; MEF=mouse embryonic fibroblast; PPM=parts per million; WCLB=whole cell lysis buffer.

7. References

Attar, N., Campos, O.A., Vogelauer, M., Cheng, C., Xue, Y., Schmollinger, S., Salwinski, L., Mallipeddi, N.V., Boone, B.A., Yen, L.*, et al.* (2020). The histone H3-H4 tetramer is a copper reductase enzyme. Science *369*, 59-64.

Berlanga, J.J., Ventoso, I., Harding, H.P., Deng, J., Ron, D., Sonenberg, N., Carrasco, L., and de Haro, C. (2006). Antiviral effect of the mammalian translation initiation factor 2alpha kinase GCN2 against RNA viruses. EMBO J *25*, 1730-1740.

Bertinato, J., and L'Abbe, M.R. (2003). Copper modulates the degradation of copper chaperone for Cu,Zn superoxide dismutase by the 26 S proteosome. J Biol Chem *278*, 35071-35078.

Bi, M., Naczki, C., Koritzinsky, M., Fels, D., Blais, J., Hu, N., Harding, H., Novoa, I., Varia, M., Raleigh, J.*, et al.* (2005). ER stress-regulated translation increases tolerance to extreme hypoxia and promotes tumor growth. EMBO J *24*, 3470-3481.

Bond, S., Lopez-Lloreda, C., Gannon, P.J., Akay-Espinoza, C., and Jordan-Sciutto, K.L. (2020). The Integrated Stress Response and Phosphorylated Eukaryotic Initiation Factor 2alpha in Neurodegeneration. J Neuropathol Exp Neurol *79*, 123-143.

Boyce, M., Bryant, K.F., Jousse, C., Long, K., Harding, H.P., Scheuner, D., Kaufman, R.J., Ma, D., Coen, D.M., Ron, D.*, et al.* (2005). A selective inhibitor of eIF2alpha dephosphorylation protects cells from ER stress. Science *307*, 935-939.

Brady, D.C., Crowe, M.S., Turski, M.L., Hobbs, G.A., Yao, X., Chaikuad, A., Knapp, S., Xiao, K., Campbell, S.L., Thiele, D.J.*, et al.* (2014). Copper is required for oncogenic BRAF signalling and tumorigenesis. Nature *509*, 492-496.

Caruano-Yzermans, A.L., Bartnikas, T.B., and Gitlin, J.D. (2006). Mechanisms of the copper-dependent turnover of the copper chaperone for superoxide dismutase. J Biol Chem *281*, 13581-13587.

Chaikuad, A., Koschade, S.E., Stolz, A., Zivkovic, K., Pohl, C., Shaid, S., Ren, H., Lambert, L.J., Cosford, N.D.P., Brandts, C.H.*, et al.* (2019). Conservation of structure, function and inhibitor binding in UNC-51-like kinase 1 and 2 (ULK1/2). Biochem J *476*, 875-887.

Chen, Y., Zhang, B., Cao, S., Huang, W., Liu, N., and Yang, W. (2018). GanDouLing combined with Penicillamine improves cerebrovascular injury via PERK/eIF2alpha/CHOP endoplasmic reticulum stress pathway in the mouse model of Wilson's disease. Biosci Rep *38*.

Chen, Y.W., Chen, K.L., Chen, C.H., Wu, H.C., Su, C.C., Wu, C.C., Way, T.D., Hung, D.Z., Yen, C.C., Yang, Y.T.*, et al.* (2010). Pyrrolidine dithiocarbamate (PDTC)/Cu complex induces lung epithelial cell apoptosis through mitochondria and ER-stress pathways. Toxicol Lett *199*, 333-340.

Cui, W., Li, J., Ron, D., and Sha, B. (2011). The structure of the PERK kinase domain suggests the mechanism for its activation. Acta Crystallogr D Biol Crystallogr *67*, 423-428.

Fischmann, T.O., Smith, C.K., Mayhood, T.W., Myers, J.E., Reichert, P., Mannarino, A., Carr, D., Zhu, H., Wong, J., Yang, R.S.*, et al.* (2009). Crystal structures of MEK1 binary and ternary complexes with nucleotides and inhibitors. Biochemistry *48*, 2661-2674.

Grasso, M., Bond, G.J., Kim, Y.-J., Alwan, K.B., Boyd, S., Dzebo, M.M., Valenzuela, S., Tsang, T., Schibrowsky, N.A., Matthews, M.L.*, et al.* (2020). Structural and molecular determinants of CCS-mediated copper activation of MEK1/2. bioRxiv, 2020.2005.2001.072124.

Grasso, M., Bond, G.J., Kim, Y.J., Boyd, S., Matson Dzebo, M., Valenzuela, S., Tsang, T., Schibrowsky, N.A., Alwan, K.B., Blackburn, N.J.*, et al.* (2021). The copper chaperone CCS facilitates copper binding to MEK1/2 to promote kinase activation. J Biol Chem *297*, 101314.

Grubman, A., and White, A.R. (2014). Copper as a key regulator of cell signalling pathways. Expert Rev Mol Med *16*, e11.

Guo, J., Cheng, J., Zheng, N., Zhang, X., Dai, X., Zhang, L., Hu, C., Wu, X., Jiang, Q., Wu, D.*, et al.* (2021). Copper Promotes Tumorigenesis by Activating the PDK1-AKT Oncogenic Pathway in a Copper Transporter 1 Dependent Manner. Adv Sci (Weinh) *8*, e2004303.

Gupta, S., Giricz, Z., Natoni, A., Donnelly, N., Deegan, S., Szegezdi, E., and Samali, A. (2012). NOXA contributes to the sensitivity of PERK-deficient cells to ER stress. FEBS Lett *586*, 4023-4030.

Harding, H.P., Zhang, Y., Bertolotti, A., Zeng, H., and Ron, D. (2000). Perk is essential for translational regulation and cell survival during the unfolded protein response. Mol Cell *5*, 897-904.

Harding, H.P., Zhang, Y., Zeng, H., Novoa, I., Lu, P.D., Calfon, M., Sadri, N., Yun, C., Popko, B., Paules, R.*, et al.* (2003). An integrated stress response regulates amino acid metabolism and resistance to oxidative stress. Mol Cell *11*, 619-633.

Hetz, C., and Papa, F.R. (2018). The Unfolded Protein Response and Cell Fate Control. Mol Cell *69*, 169-181.

Kardos, J., Heja, L., Simon, A., Jablonkai, I., Kovacs, R., and Jemnitz, K. (2018). Copper signalling: causes and consequences. Cell Commun Signal *16*, 71.

Krishnamoorthy, L., Cotruvo, J.A., Jr., Chan, J., Kaluarachchi, H., Muchenditsi, A., Pendyala, V.S., Jia, S., Aron, A.T., Ackerman, C.M., Wal, M.N.*, et al.* (2016). Copper regulates cyclic-AMP-dependent lipolysis. Nat Chem Biol *12*, 586-592.

Liu, Z., Lv, Y., Zhao, N., Guan, G., and Wang, J. (2015). Protein kinase R-like ER kinase and its role in endoplasmic reticulum stress-decided cell fate. Cell Death Dis *6*, e1822.

Lu, P.D., Jousse, C., Marciniak, S.J., Zhang, Y., Novoa, I., Scheuner, D., Kaufman, R.J., Ron, D., and Harding, H.P. (2004). Cytoprotection by pre-emptive conditional phosphorylation of translation initiation factor 2. EMBO J *23*, 169-179.

Magistrato, A., Pavlin, M., Qasem, Z., and Ruthstein, S. (2019). Copper trafficking in eukaryotic systems: current knowledge from experimental and computational efforts. Curr Opin Struct Biol *58*, 26-33.

Noack, J., Brambilla Pisoni, G., and Molinari, M. (2014). Proteostasis: bad news and good news from the endoplasmic reticulum. Swiss Med Wkly *144*, w14001.

Opazo, C.M., Lotan, A., Xiao, Z., Zhang, B., Greenough, M.A., Lim, C.M., Trytell, H., Ramírez, A., Ukuwela, A.A., Mawal, C.H.*, et al.* (2021). Nutrient copper signaling promotes protein turnover by allosteric activation of ubiquitin E2D conjugases. bioRxiv, 2021.2002.2015.431211.

Shacham, T., Patel, C., and Lederkremer, G.Z. (2021). PERK Pathway and Neurodegenerative Disease: To Inhibit or to Activate? Biomolecules *11*.

Tan, S., Somia, N., Maher, P., and Schubert, D. (2001). Regulation of antioxidant metabolism by translation initiation factor 2alpha. J Cell Biol *152*, 997-1006.

Tsang, T., Davis, C.I., and Brady, D.C. (2021). Copper biology. Curr Biol *31*, R421-R427.

Tsang, T., Posimo, J.M., Gudiel, A.A., Cicchini, M., Feldser, D.M., and Brady, D.C. (2020). Copper is an essential regulator of the autophagic kinases ULK1/2 to drive lung adenocarcinoma. Nat Cell Biol.

Turski, M.L., Brady, D.C., Kim, H.J., Kim, B.E., Nose, Y., Counter, C.M., Winge, D.R., and Thiele, D.J. (2012). A novel role for copper in Ras/mitogen-activated protein kinase signaling. Mol Cell Biol *32*, 1284-1295.

Urra, H., Dufey, E., Lisbona, F., Rojas-Rivera, D., and Hetz, C. (2013). When ER stress reaches a dead end. Biochim Biophys Acta *1833*, 3507-3517.

Walter, P., and Ron, D. (2011). The unfolded protein response: from stress pathway to homeostatic regulation. Science *334*, 1081-1086.

Wek, R.C., Jiang, H.Y., and Anthony, T.G. (2006). Coping with stress: eIF2 kinases and translational control. Biochem Soc Trans *34*, 7-11.

Yang, Q., Wang, Y., Yang, Q., Gao, Y., Duan, X., Fu, Q., Chu, C., Pan, X., Cui, X., and Sun, Y. (2017). Cuprous oxide nanoparticles trigger ER stress-induced apoptosis by regulating copper trafficking and overcoming resistance to sunitinib therapy in renal cancer. Biomaterials *146*, 72-85.